Cerebral Cortex, May 2019;29: 1875–1888

doi: 10.1093/cercor/bhy067
Advance Access Publication Date: 13 April 2018
Original Article

ORIGINAL ARTICLE

Adult-Onset Hearing Impairment Induces Layer-Specific Cortical Reorganization: Evidence of Crossmodal Plasticity and Central Gain Enhancement

Ashley L. Schormans, Marei Typlt and Brian L. Allman

Department of Anatomy and Cell Biology, Schulich School of Medicine and Dentistry, University of Western Ontario, London, Ontario, Canada N6A 5C1

Address correspondence to Brian L. Allman, Department of Anatomy and Cell Biology, Schulich School of Medicine and Dentistry, University of Western Ontario, 1151 Richmond Street, London, Ontario, Canada N6A 5C1. Email: brian.allman@schulich.uwo.ca

Abstract

Adult-onset hearing impairment can lead to hyperactivity in the auditory pathway (i.e., central gain enhancement) as well as increased cortical responsiveness to nonauditory stimuli (i.e., crossmodal plasticity). However, it remained unclear to what extent hearing loss-induced hyperactivity is relayed beyond the auditory cortex, and thus, whether central gain enhancement competes or coexists with crossmodal plasticity throughout the distinct layers of the audiovisual cortex. To that end, we investigated the effects of partial hearing loss on laminar processing in the auditory, visual and audiovisual cortices of adult rats using extracellular electrophysiological recordings performed 2 weeks after loud noise exposure. Current-source density analyses revealed that central gain enhancement was not relayed to the audiovisual cortex (V2L), and was instead restricted to the granular layer of the higher order auditory area, AuD. In contrast, crossmodal plasticity was evident across multiple cortical layers within V2L, and also manifested in AuD. Surprisingly, despite this coexistence of central gain enhancement and crossmodal plasticity, noise exposure did not disrupt the responsiveness of these neighboring cortical regions to combined audiovisual stimuli. Overall, we have shown for the first time that adult-onset hearing impairment causes a complex assortment of intramodal and crossmodal changes across the layers of higher order sensory cortices.

Key words: audiovisual processing, cortical plasticity, hearing loss, lateral extrastriate visual cortex, noise exposure

Introduction

Hearing impairment is a highly prevalent neurological problem, affecting ~16% of adults in the USA (Agrawal et al. 2008; Lin et al. 2011). Furthermore, according to the Centers for Disease Control and Prevention, nearly 10 million Americans suffer from hearing loss related to excessive noise exposure, and each year ~22 million workers are exposed to noise levels that could lead to hearing impairment. Consistent with noninvasive studies on hearing-impaired individuals, preclinical research using animal models has revealed that noise-induced hearing loss causes considerable neural plasticity throughout the central auditory pathway. For example, the loss of sensory output from the damaged cochlea leads to a paradoxical increase in neural activity at the successive relay nuclei, ultimately manifesting as hyperactivity in the core auditory cortex (i.e., central gain enhancement) (Popelar et al. 1987, 1995, 2008; Salvi et al. 1990, 2000). Numerous studies have investigated the various cochlear insults that can lead to an increase in central gain, as well as the putative perceptual consequences (e.g., tinnitus? hyperacusis?) (for review, see Auerbach et al. 2014). At present, however, it remains unclear to what extent this deprivation-induced hyperactivity in the core auditory cortex is relayed to higher order, multisensory areas of the brain that are

tasked with integrating converging inputs from different sensory modalities (e.g., hearing and vision).

This issue of whether central gain enhancement in the auditory system disrupts audiovisual integration is particularly relevant given that hearing impairment not only affects how sound is processed but can also alter cortical responsiveness to non-auditory stimuli (i.e., crossmodal plasticity). It has long been suggested that the loss of one sense (e.g., hearing) allows for the invasion of the deprived cortical areas by the spared senses (e.g., vision) (Rauschecker 1995). Although this suggestion is consistent with crossmodal plasticity observed in deaf humans (Finney et al. 2001, 2003; Doucet et al. 2006; Auer et al. 2007; Vachon et al. 2013) as well as early- and late-onset profound hearing loss in animal models (Kral et al. 2003; Hunt et al. 2006; Allman et al. 2009; Meredith and Lomber 2011), it is reasonable to question whether it would be at odds with an increase in central gain that occurs in the core auditory cortex after moderate hearing loss. In such cases when some residual hearing is preserved, the core auditory cortex shows evidence of tonotopic reorganization, increased neuronal synchrony, and hyperactivity not quiescence (Komiya and Eggermont 2000; Popescu and Polley 2010; Engineer et al. 2011; Meredith and Keniston et al. 2012; Meredith and Allman et al. 2012; Salvi et al. 2000); factors which could alter its susceptibility to crossmodal plasticity. To date, numerous studies have separately examined the emergence of central gain enhancement or crossmodal plasticity, but no studies have determined whether these 2 phenomena compete or coexist in the neighboring regions of auditory, visual and audiovisual cortices following partial hearing loss. This possibility of regional specificity is particularly relevant because it is known that not all areas of the auditory cortex show the same degree of crossmodal plasticity in profoundly deaf subjects (Kral et al. 2003; Lomber et al. 2010; Meredith et al. 2011).

Studies in both humans and animal models have shown that even a modest hearing impairment is sufficient to induce crossmodal plasticity. For example, visual and audiovisual-evoked potentials were altered in adults with mild-moderate hearing loss compared with age-matched controls (Musacchia et al. 2009; Campbell and Sharma 2014), and these hearing-impaired subjects showed an increased responsiveness to visual stimuli in more temporal cortical regions (Campbell and Sharma 2014). Consistent with these results, adult-onset hearing impairment increased visual processing in the core auditory cortex of ferrets (Meredith and Keniston et al. 2012) as well as the audiovisual cortex of rats (Schormans and Typlt et al. 2017). However, because these previous studies did not segregate their results according to the depth of the recording penetrations throughout the cortical mantle, it remains uncertain whether partial hearing loss differentially affects sensory processing across the cortical layers within the higher order sensory areas; findings that could provide important insight into the contributions of thalamocortical versus intracortical processing in the manifestation of central gain enhancement and crossmodal plasticity.

In the present study, we conducted the first investigation into how adult-onset hearing loss alters auditory, visual and audiovisual processing across the distinct layers of higher order sensory cortices. In doing so, we sought to reveal the extent that deprivation-induced hyperactivity in the auditory pathway is relayed beyond the core auditory cortex, and thus, whether central gain enhancement competes or coexists with crossmodal plasticity in the audiovisual cortex following partial hearing loss in adulthood. Two weeks after loud noise exposure, adult rats were anesthetized and extracellular electrophysiological recordings were performed in 4 neighboring cortical regions: the primary visual cortex (V1), the multisensory zone of the lateral extrastriate visual cortex (V2L-Mz), the auditory zone of the lateral extrastriate visual cortex (V2L-Az), and the dorsal auditory cortex (AuD; a higher order auditory area). By inserting a 32-channel linear electrode array orthogonal to the pial surface, laminar processing was assessed in each cortical region in response to auditory, visual and combined audiovisual stimuli by sampling the local field potential (LFP) across the entire cortical thickness. Current-source density (CSD) analysis was then applied to these LFP data to determine the effect of partial hearing loss on central gain enhancement and crossmodal plasticity at the level of postsynaptic potentials. Ultimately, this novel approach allowed us to reveal that adult-onset hearing impairment causes a complex assortment of intramodal and crossmodal changes across the layers of neighboring regions of the higher order sensory cortices.

Methods

Animals

In total, 17 adult male Sprague-Dawley rats aged 110 ± 3 days (body mass: 421 ± 12.6 g; Charles River Laboratories, Inc., Wilmington, MA) were used in this study, and were housed on a 12-h light-dark cycle with food and water ad libitum. All experimental procedures were approved by the University of Western Ontario Animal Care and Use Committee and were in accordance with the guidelines established by the Canadian Council of Animal Care.

Hearing Assessment

Consistent with an established protocol (Schormans and Typlt et al. 2017), hearing sensitivity was assessed with the auditory brainstem response (ABR), which was performed in a double-walled sound-attenuating chamber (MDL 6060 ENV, Whisper Room Inc, Knoxville, TN). Rats were anesthetized with ketamine (80 mg/kg; IP) and xylazine (5 mg/kg; IP), and subdermal electrodes (27 gauge; Rochester Electro-Medical, Lutz, FL) were positioned at the vertex, over the right mastoid and on the back. Throughout the hearing assessment procedure, body temperature was maintained at ~37 °C using a homeothermic heating pad (507220F; Harvard Apparatus, Kent, UK).

Auditory stimuli consisting of a click (0.1 ms) and 2 tones (4 kHz and 20 kHz; 5 ms duration and 1 ms rise/fall time) were generated using Tucker-Davis Technologies RZ6 processing module sampled at 100 kHz (TDT, Alachua, FL). The auditory stimuli were delivered by a speaker (MF1; TDT) positioned 10 cm from the animal's right ear while the left ear was occluded with a custom foam ear plug. All stimuli were presented 1000 times (21 times/s) at decreasing intensities from 90 to 10 dB sound pressure level (SPL). Near threshold, successive steps were decreased to 5 dB SPL, and each sound level was presented twice in order to best determine ABR threshold using the criteria of just noticeable deflection of the averaged electrical activity within the 10-ms time window (Popelar et al. 2008). Sound stimuli used for the ABR, noise exposure and electrophysiological recordings were calibrated with custom MATLAB software (The Mathworks, Natick, MA) using a ¼-inch microphone (2530; Larson Davis, Depew, NY) and preamplifier (2221; Larson Davis). The auditory-evoked activity was collected using a low-impedance headstage (RA4L1; TDT), then preamplified and digitized (RA16SD Medusa preamp; TDT) and sent to a RZ6 processing module via a fiber optic cable.

Rats in the control group ($n = 8$) underwent an ABR to assess their hearing levels, followed immediately by an in vivo extracellular electrophysiological recording experiment. Noise exposed rats ($n = 9$) underwent a baseline hearing assessment, followed by exposure to a loud broadband noise (see below for details). Two weeks following the noise exposure, a final hearing assessment was performed, after which the same electrophysiological recording experiment was completed as in control rats.

Noise Exposure

Rats were bilaterally exposed to a broadband noise (0.8–20 kHz) for 2 h at 120 dB SPL while under ketamine (80 mg/kg; IP) and xylazine (5 mg/kg; IP), and body temperature was maintained at ~37 °C using a homeothermic heating pad. This broadband noise exposure protocol was chosen because it was found to be effective at inducing a permanent threshold shift as assessed using the ABR as well as persistent changes in the auditory cortex (Popelar et al. 2008) and the audiovisual cortex (Schormans and Typlt et al. 2017). The broadband noise was generated with TDT software (RPvdsEx) and hardware (RZ6), and delivered by a super tweeter (T90A; Fostex, Tokyo, Japan) which was placed 10 cm in front of the rat.

Surgical Procedure

Following the final hearing assessment, each rat was maintained under ketamine/xylazine anesthesia, the foam earplug was removed from the left ear, and the animal was fixed in a stereotaxic frame with blunt ear bars. The absence of a pedal withdrawal reflex was an indication of anesthetic depth, and supplemental doses of ketamine/xylazine were administered (IM) as needed. A midline incision was made in the skin of the scalp, and the dorsal aspect of the skull was cleaned with a scalpel blade. The left temporalis muscle was reflected to provide access to the temporal bone overlying the auditory and audiovisual cortices. A stereotaxic manipulator was used to measure 6 mm caudal to bregma, which represents an approximate location of the lateral extrastriate visual cortex (V2L) (Wallace et al. 2004; Hirokawa et al. 2008; Schormans and Typlt et al. 2017; Xu et al. 2014), and a mark was made on the skull for later drilling. Additional marks were made on the temporal bone at 1, 2, and 3 mm ventral of the top of the skull (i.e., dorsal/ventral measurements were zeroed on the sagittal suture at 6 mm caudal to bregma; the most dorsal aspect of the skull). A stainless steel screw was inserted in the left frontal bone to serve as an anchor for the headpost and an electrical ground. A craniotomy (2 × 5 mm; 5–7 mm caudal to bregma) was performed in the left temporal and parietal bone in order to expose the auditory, visual and audiovisual cortices. A headpost was fastened to the skull with dental acrylic on the right frontal bone, and the right ear bar was removed to allow free-field auditory stimulation of the right ear during the electrophysiological recordings in the contralateral cortex. The rat was held in position throughout the entire duration of the experiment within the stereotaxic frame using the left ear bar and the headpost.

Electrophysiological Recordings

At least 4 recording penetrations were performed in each animal. At each of the recording locations (described in detail below), a 32-channel linear electrode array was inserted perpendicular to the cortex through a small slit in the dura using a hydraulic microdrive (FHC; Bowdoin, ME). The array consisted of 32 iridium microelectrodes equally spaced 50 µm apart on a 50-µm-thick shank, spanning 1550 µm (A1x32-10 mm-50-177-A32; NeuroNexus Technologies, Ann Arbor, MI). Prior to insertion in the cortex, the electrode array was coated in DiI cell-labeling solution (V22885; Molecular Probes, Inc., Eugene, OR) to allow for histological reconstruction of electrode penetrations. Initially, the electrode array was advanced into the cortex using a high-precision stereotaxic manipulator to penetrate the pia mater, and then withdrawn to the cortical surface. The hydraulic microdrive was then used to slowly advance the electrode array until it reached a depth of −1500 µm. For each cortical region, slight adjustments to depth were made based on a characteristic sharp negative peak of the LFP to the preferred stimulus (i.e., the unimodal stimulus that evoked the largest response) (typically −350 to −450 µm depth below the pial surface) (Stolzberg et al. 2012). Once at this depth (control: −396 ± 11 µm; noise exposed: −377 ± 13 µm), the electrode was allowed to settle in place for 45 minutes before electrophysiological recordings commenced. Electrophysiological signals were acquired using TDT System 3 (TDT, Alachua, FL), and LFP activity was continuously acquired (digitally resampled at approximately 1000 Hz) and bandpass filtered online at 1–300 Hz.

In all rats, recordings were completed within 4 brain regions: (1) the primary visual cortex (V1; corresponding to the 1 mm ventral of the marking on the skull using our measurements), (2) the multisensory zone of the lateral extrastriate visual cortex (V2L-Mz; 2 mm ventral); (3) the auditory zone of the lateral extrastriate visual cortex (V2L-Az; 2.5 mm ventral); and finally, (4) the dorsal auditory cortex (AuD; 3 mm ventral). Figure 1 shows a schematic of the location for each of the 4 penetrations per animal from all of the electrophysiological experiments.

Sensory Stimulation

At each of the recording locations, a quantitative multisensory paradigm was performed, which included computer-triggered auditory and visual stimuli presented alone or in combination. Auditory stimuli consisted of noise bursts (1–32 kHz; 50 ms duration) from a speaker positioned 10 cm from the right pinna on a 30° angle to the right of midline. For each rat, the auditory stimulus was presented 40 dB above its click threshold (control: 68.3 ± 1.1 dB SPL; noise exposed: 82.5 ± 1.7 dB SPL). Visual stimuli consisted of light flashes (15 lux; 50 ms duration) from an LED (diameter: 0.8 cm) positioned adjacent to the speaker (i.e., 10 cm from the right eye). The intensity of the visual stimulus was determined using a LED light meter (Model LT45, Extech Instruments, Nashua, NH). During the combined stimulus condition, the visual stimulus was presented 30 ms prior to the auditory stimulus. Consistent with previous studies (Allman and Meredith 2007; Allman et al. 2008; Meredith and Allman 2009, 2015), this timing offset maximized the potential for observing a multisensory interaction because it compensated for differences in latency for each modality and helped ensure that both stimuli arrived simultaneously within the temporal cortex. In total, the 3 stimuli conditions were presented in a randomized order, separated by an interstimulus interval of 3–5 s, and each condition was presented 50 times.

Current Source Density Analysis

The CSD provides a measure of the total current density that enters or leaves the extracellular space through the cell membrane (Mitzdorf 1985; Einevoll et al. 2013). A one-dimensional CSD analysis was applied to the mean LFPs recorded simultaneously across the entire cortical thickness using the following formula:

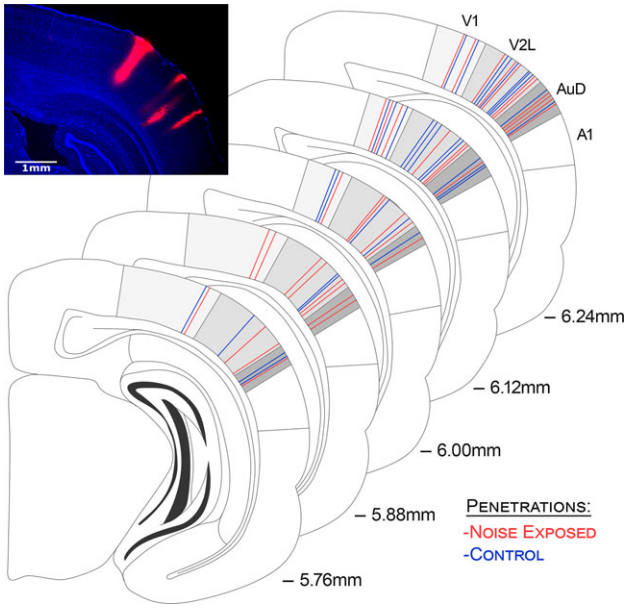

Figure 1. Electrode penetrations across all recording locations within the primary visual cortex (V1), the lateral extrastriate visual cortex (V2L), and the dorsal auditory cortex (AuD). The stained image shows a representative coronal section demonstrating the location of recording penetrations 6.0 mm caudal of bregma. Prior to being inserted into the cortex, the electrode was coated in DiI cell-labeling solution allowing for post-experiment histological reconstruction of the penetrations. Note that despite not being visible on this single section, it was confirmed in neighboring rostral/caudal sections that all penetrations did indeed span the full distance of the cortical mantle. The schematic shows a reconstruction of all of the recording penetrations for control (blue; $n = 32$) and noise exposed (red; $n = 36$) experiments spanning 5.76–6.24 mm caudal of bregma. In accordance with Paxinos and Watson (2007), the most dorsal recording penetrations were located in the V1, whereas the most ventral recording penetrations were in the AuD. One penetration per rat was located in each of these predominantly unisensory areas. Two penetrations per rat targeted the multisensory area, the lateral extrastriate visual cortex (V2L) (Schormans and Typlt et al. 2017); one penetration in the more dorsal-positioned, multisensory zone of the V2L (V2L-Mz), and the other in the auditory zone (V2L-Az).

$$CSD \approx -\frac{\Phi(z + n\Delta z) - 2\Phi(z) + \Phi(z - n\Delta z)}{(n\Delta z)^2} \quad (1)$$

where, Φ is the LFP, z is the spatial coordinate, Δz is the inter-electrode spacing ($\Delta z = 50\,\mu m$), and n is the differentiation grid ($n = 4$) (Nicholson and Freeman 1975; Mitzdorf and Singer 1977, 1980; Freeman and Singer 1983; Mitzdorf 1985). This CSD equation approximates the second derivative of the LFPs at each point in time across electrode sites, which is due to the transmembrane current sources or sinks. A 3-point Hamming filter was applied in order to smooth LFPs across channels before computing the CSD, as described by Stolzberg et al. (2012). In accordance with previous studies (Nicholson and Freeman 1975; Mitzdorf and Singer 1977, 1980; Freeman and Singer 1983; Mitzdorf 1985; Stolzberg et al. 2012), current sinks were positive in amplitude, and sources were negative.

CSD analysis reveals the net flow of ions into and out of the neural tissue; sinks represent the flow of positive ions into the neural tissue from the extracellular space, which corresponds to events such as active excitatory synaptic populations and axonal depolarization (Kral and Eggermont 2007; Happel et al. 2010). Current sources are reflective of passive return currents, and are indicative of repolarization and possibly inhibition of the neighboring tissue (Mitzdorf 1985; Kral and Eggermont 2007; Happel et al. 2010; Einevoll et al. 2013; Szymanski et al. 2009). In the present study, only CSD sinks were analyzed at each of the 4 recording locations and for each stimulus condition. Across all cortical regions, sinks were identified as being at least 3 standard deviations above the mean voltage measured during the 70 ms before either stimulus was presented. Within the majority of recording locations, prominent sinks were identified in the granular ($-300\,\mu m$ < depth ≥ $-750\,\mu m$) and infragranular-upper layers ($-750\,\mu m$ < depth ≥ $-1200\,\mu m$). Additional sinks of longer latency were observed in supragranular (depth ≥ $-350\,\mu m$) and infragranular-lower layers (depth < $-1200\,\mu m$) (Fig. 2A).

To assess changes across the cortical layers, CSD waveforms were extracted from the depth that demonstrated the highest amplitude within an individual sink (i.e., peak amplitude). For each of the 4 identified sinks, the peak amplitude was derived from a single depth in order to account for individual sink components that spanned various depths (e.g., extended beyond or were narrower than the space defined above). The peak amplitude was computed for all stimulus conditions. All calculations were performed using custom Matlab scripts.

Average Rectified CSD Analysis

To determine the overall strength of postsynaptic currents in each of the cortical areas, the average rectified CSD (AVREC) measure was applied to the CSD analysis (Schroeder et al. 1997, 2001; Happel et al. 2010; Stolzberg et al. 2012). Although rectification results in a loss of information about the direction of the transmembrane current flow, the AVREC waveform provides a measure of the temporal pattern of the overall strength of the postsynaptic currents (Givre et al. 1994; Schroeder et al. 1998; Happel et al. 2010). The AVREC was calculated by averaging the absolute values of the CSD across all channels (Eq. 2).

$$\text{AVREC} = \frac{\sum_{i=1}^{n} |CSD_i|(t)}{n} \quad (2)$$

where, CSD refers to Eq. 1, n refers to the number of channels, and t refers to the time point index. To complete a quantitative analysis of the AVREC, peak amplitude was calculated for all cortical areas and stimulus conditions within the first 200 ms from the onset of the visual stimulus.

Statistics

Statistical analyses were conducted on the data using various procedures, including repeated-measures analysis of variance (ANOVA), one-way ANOVA or paired/unpaired t-tests depending on the comparison of interest (see Results for details of each specific comparison). In several cases, statistical analyses commenced with a 3-way repeated-measures ANOVA, and following confirmation of significant interactions, subsequent 2-way repeated-measures ANOVAs were performed. All statistical comparisons used an alpha value of 0.05, and Bonferroni post hoc corrections were performed when appropriate. GraphPad Prism (GraphPad Software Inc.) and MATLAB (2012b; The Mathworks) were used for graphical display, and SPSS (Version 20, IBM Corporation) software was used for the various statistical analyses. Throughout the text and figures, data are presented as the mean values ± standard error of the mean (SEM).

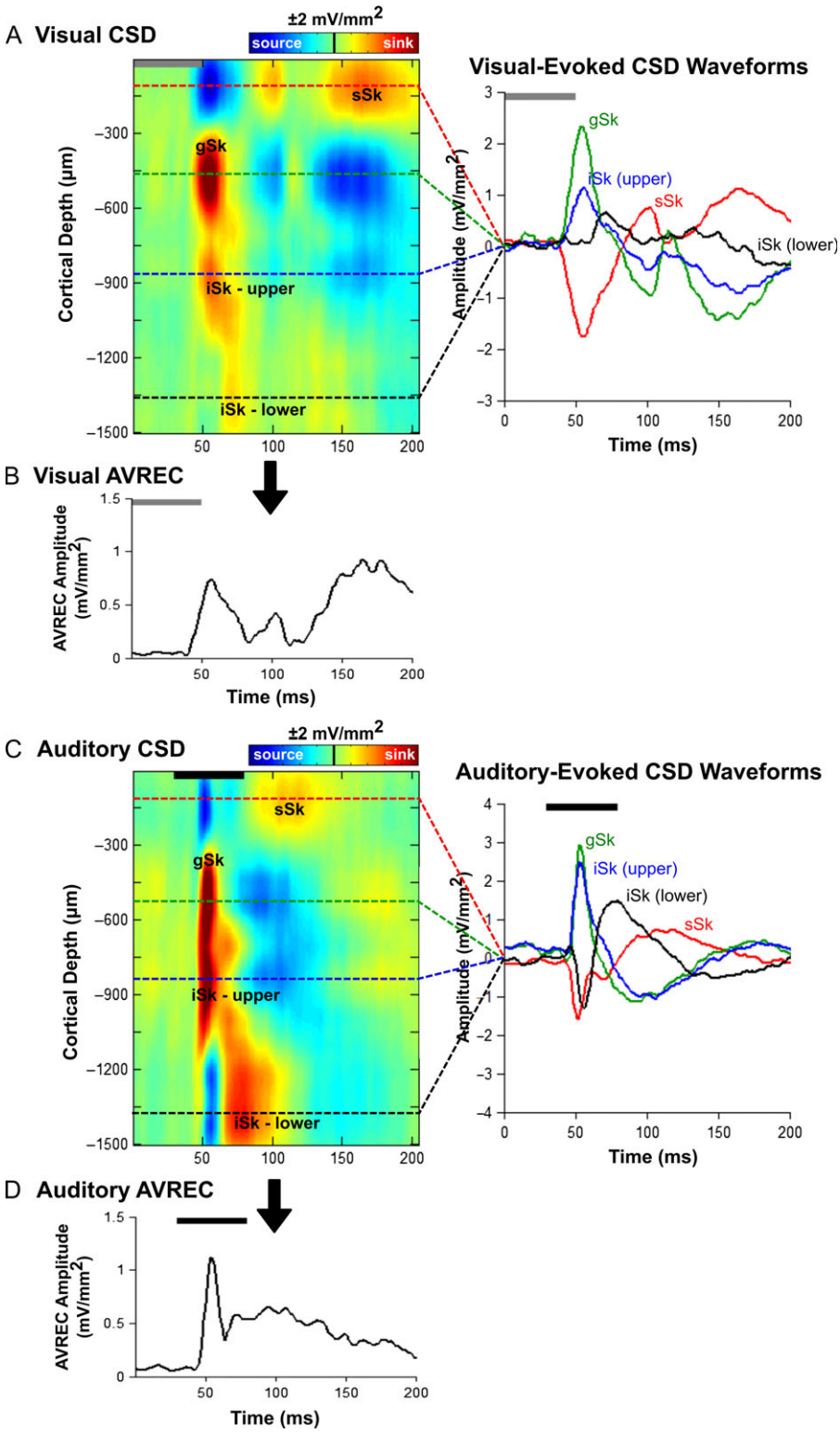

Figure 2. Visual- and auditory-evoked current source density (CSD) profiles within the multisensory zone of the lateral extrastriate visual cortex (V2L-Mz). (*A*) Representative CSD profile (left) and extracted CSD waveforms (right) from a control rat in response to a visual stimulus (50 ms LED flash at 15 lux, denoted by the grey bar). Prominent current sinks (red) are reflective of a depolarization of neurons in the surrounding cortical region, whereas prominent current sources (blue) reflect a repolarization of neurons in the surrounding cortical regions. As shown in the CSD waveforms, the supragranular (sSk, red), granular (gSk, green), infragranular-upper (iSk upper, blue) and infragranular-lower (iSk lower, black) responses (sinks are positive, sources are negative) were extracted from the electrode showing the highest amplitude for each of the individual sinks (denoted by the dashed lines on the CSD images). (*B*) Average rectified current source density (AVREC) analysis derived from the CSD profiles in (*A*) in response to a visual stimulus. (*C*) Representative CSD profile (left) and extracted CSD waveforms (right) from a control rat in response to an auditory stimulus (50 ms noise burst at 40 dB above click threshold, denoted by the black bar). (*D*) Average rectified current source density (AVREC) analysis derived from the CSD profiles in (*C*) in response to an auditory stimulus.

Histology

At the completion of the electrophysiological experiment, the rats were injected with sodium pentobarbital (100 mg/kg; IP) in preparation for exsanguination via transcardial perfusion of 0.1 M phosphate buffer (PB), followed by 4% paraformaldehyde. Using a microtome (HM 430/34; Thermo Scientific, Waltham, MA), frozen sections (50 μm) were cut in the coronal plane and collected serially. The sections were mounted in fluorescent DAPI mounting medium (F6057 Fluoroshield™ with DAPI; Sigma, St. Louis, MO) and coverslipped. Because the recording electrode array was coated in fluorescent DiI cell-labeling solution prior to insertion into the cortex, it was possible to reconstruct the location and depth of the 4 recording penetrations in each rat (Fig. 1). Sections containing the recording penetrations were imaged with an Axio Vert A1 inverted microscope (Carl Zeiss Microscopy GmbH, Jena, Germany), and ZEN imaging software was used to reconstruct the location of each recording penetration.

Results

Noise-Induced Hearing Loss

To determine the effect of noise exposure on hearing sensitivity, the ABR threshold of the click, 4 and 20 kHz stimuli were compared at baseline versus 2 weeks postnoise in the noise exposed rats ($n = 9$). A 2-way repeated-measures ANOVA ($F[1,8] = 24.9$, $P < 0.001$) with Bonferroni post hoc testing (adjusted P-value = 0.017) revealed that noise exposure caused a significant increase in the ABR threshold of the click (prenoise 26.7 ± 1.2 dB SPL vs. postnoise 40.6 ± 1.6, $P < 0.001$), 4 kHz stimulus (prenoise 22.8 ± 1.7 vs. postnoise 43.9 ± 3.2, $P < 0.001$), and 20 kHz stimulus (prenoise 12.8 ± 1.7 vs. postnoise 36.7 ± 7.0, $P < 0.017$) (Fig. 3A). As expected at baseline, there was no difference in hearing sensitivity between the control and noise exposed rats for any of the stimuli (one-way ANOVA; $P > 0.05$) (Fig. 3A).

In addition to determining the ABR thresholds to the various stimuli, the amplitude of the first wave in response to the 90 dB SPL click stimulus was used to assess the level of damage to the cochlear hair cell afferents caused by the noise exposure (Kujawa and Liberman 2009). When compared with baseline, the noise exposure resulted in a 55.6 ± 5.9% reduction of wave I amplitude measured 2 weeks later (prenoise 1.67 ± 0.1 μV vs. postnoise 0.73 ± 0.09 μV, $P < 0.001$, paired t-test), whereas the baseline wave I amplitude in the noise exposed rats was consistent with that of controls (1.5 ± 0.04 μV, $P = 0.17$, unpaired t-test) (Fig. 3B).

The sound intensity of the auditory stimulus (50 ms noise burst; 1–32 kHz) used in the electrophysiological experiments was adjusted for each rat to control for individual differences in hearing sensitivity. All rats were presented with an auditory stimulus that was 40 dB SPL above their ABR click threshold. Consequently, to account for their noise-induced hearing loss (Fig. 3A), the noise exposed rats were presented louder auditory stimulation than the controls during the electrophysiological experiment (noise exposed 81.3 ± 1.6 dB SPL vs. control 68.3 ± 0.9 dB SPL, $P < 0.001$, unpaired t-test).

Response Profile of Auditory, Visual, and Audiovisual Cortices

The present study sought to characterize the effects of adult-onset hearing loss on laminar processing in auditory, visual and multisensory cortical areas. To that end, cortical plasticity throughout the distinct layers was investigated using analyses

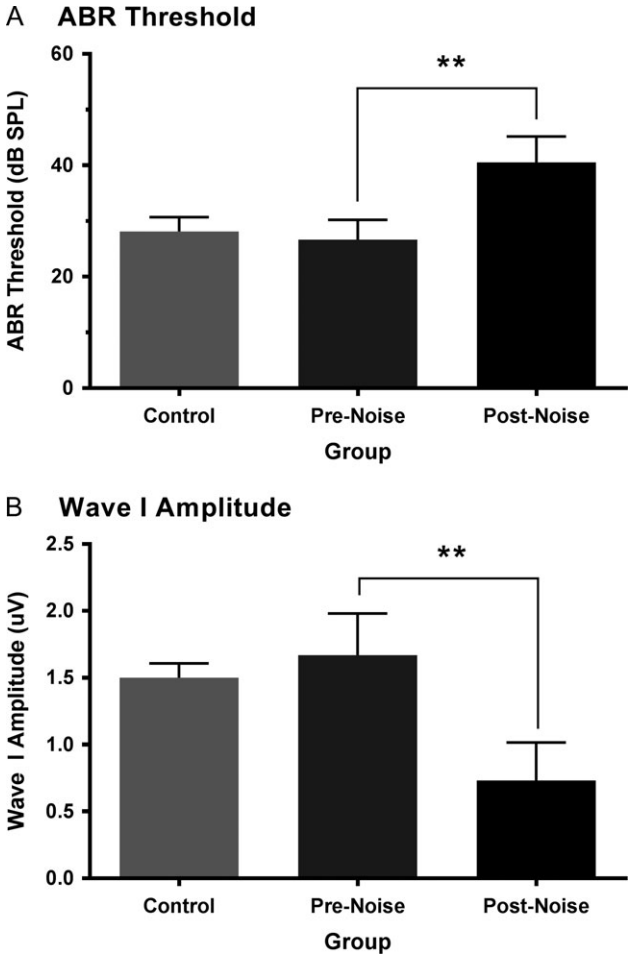

Figure 3. Assessment of the auditory brainstem response (ABR) to a click stimulus in control and noise exposed rats. ABR threshold (*A*) and amplitude of the first wave of the evoked response (*B*) to a click stimulus (0.1 ms) were assessed in control rats, as well as rats before (pre) and 2 weeks after (post) exposure to a loud broadband noise (0.8–20 kHz for 2 h at 120 dB SPL). At baseline, the ABR click threshold and wave I amplitude did not differ between the control and noise exposed rats ($P > 0.05$). Compared with their prenoise values, the rats in the noise exposure group showed a significant increase in their ABR threshold (**$P < 0.001$) and a decrease in their wave I amplitude (**$P < 0.001$) 2 weeks postnoise exposure. Values are mean ± SEM for the control ($n = 8$) and noise exposed ($n = 9$) groups.

of the CSD sink amplitude as well as AVREC peak amplitude in response to auditory, visual and combined audiovisual stimuli. Guided by stereotaxic coordinates (Paxinos and Watson (2007)) and previous studies in the rat (Barth et al. 1995; Wallace et al. 2004; Hirokawa et al. 2008; Schormans and Typlt et al. 2017; Xu et al. 2014), 32-channel laminar recordings were performed in: (1) the primary visual cortex (V1); (2) the multisensory zone of the lateral extrastriate visual cortex (V2L-Mz); (3) the auditory zone of the lateral extrastriate visual cortex (V2L-Az); and (4) the dorsal auditory cortex (AuD) (Fig. 1).

In order to designate a given penetration to a particular cortical region for subsequent analysis, we relied on extensive pilot testing and stereotaxic consistency between experiments. In control rats, histological verification of each recording penetration was combined with an assessment of the response profile observed at that location to determine its designation. For example, in contrast to the V2L-Mz, the more ventral-positioned V2L-Az was more responsive to auditory than visual stimulation in control rats; findings

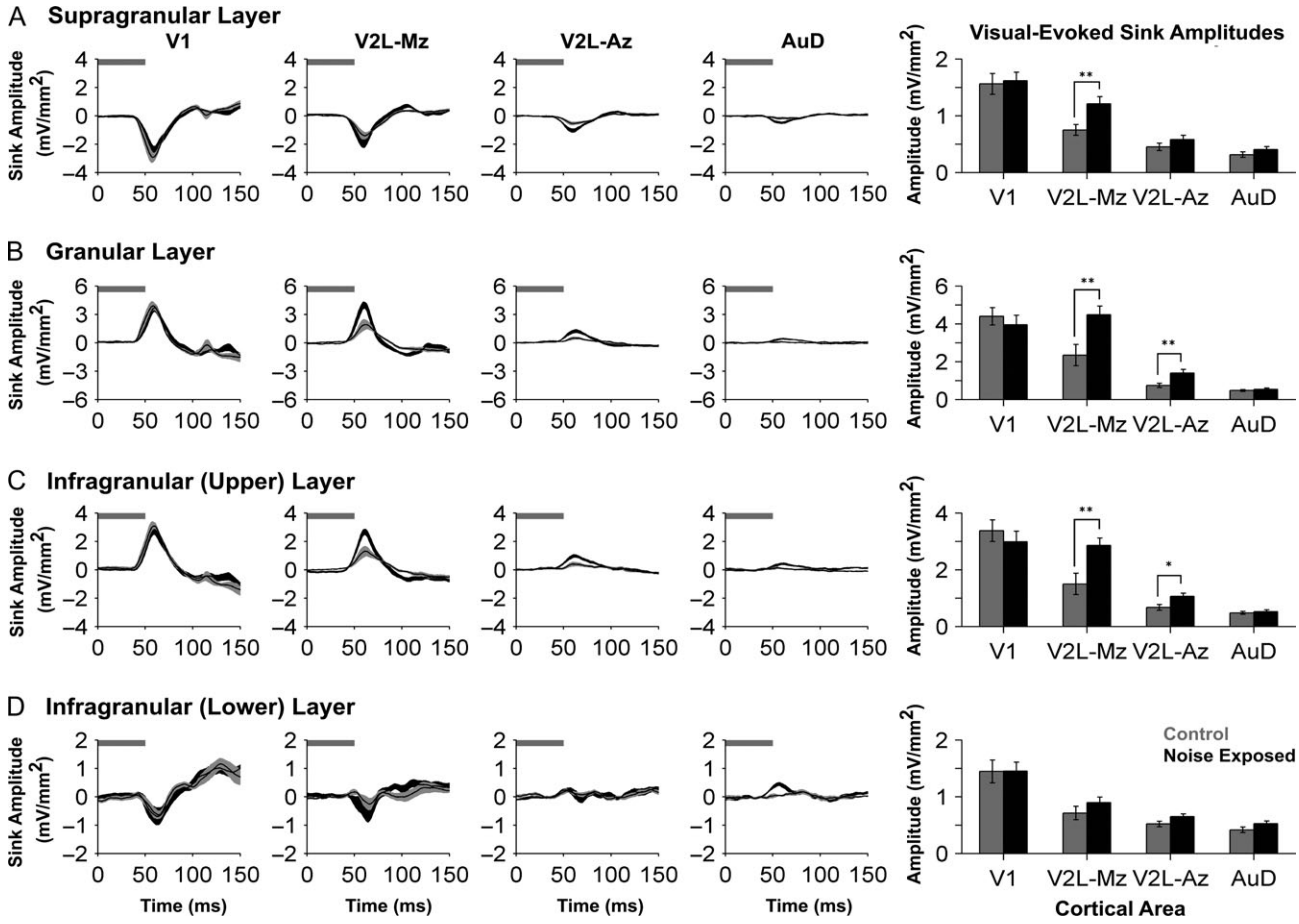

Figure 4. Increased visual responsiveness occurred across the cortical layers within higher order sensory regions. Averaged CSD waveforms from supragranular (*A*), granular (*B*), infragranular-upper (*C*), and infragranular-lower (*D*) layers within all recordings locations (i.e., V1, V2L-Mz, V2L-Az, and AuD; from left to right). Horizontal grey bar denotes the visual stimulus and the dark lines represent the group mean and shading represents the SEM for the noise exposed (dark grey; $n = 9$) and control (light grey; $n = 8$) groups. Note that in order to display the changes that occurred within each of the cortical layers, each *y*-ordinate is specific to the waveform profile for that layer. An analysis of sink amplitudes within each cortical layer (see bar graphs on the far right) shows a significant increase in visual responsiveness with the multisensory zone of V2L (V2L-Mz) across most cortical layers. This evidence of hearing loss-induced crossmodal plasticity was also present in the granular ($P < 0.01$) and the infragranular-upper layer ($P < 0.01$) of the auditory zone of V2L (V2L-Az). Values are mean ± SEM for the noise exposed ($n = 9$) and control ($n = 8$) groups. *$P < 0.05$; **$P < 0.013$.

which were consistent with our previous work using nonlaminar recordings and high-density mapping (Schormans and Typlt et al. 2017). Furthermore, the V2L-Az in control rats could be differentiated from its neighboring region, the AuD, because of consistent differences in the amplitude of the auditory-evoked AVREC (V2L-Az 2.2 ± 0.3 mV/mm^2 vs. AuD 1.5 ± 0.1 mV/mm^2). Finally, unlike in the AuD, recordings in the V2L-Az of control rats demonstrated mild visual activation observed in the AVREC peak amplitudes. Importantly, once the boundaries of the 4 cortical regions were established in the control rats, the recording penetrations reconstructed from the noise exposed rats could be designated according to their proximity to these boundaries. Ultimately, in control rats, V1 and AuD were considered predominantly unisensory areas, whereas the audiovisual cortex was comprised of 2 regions within the lateral extrastriate visual cortex (V2L-Mz and V2L-Az) (Schormans and Typlt et al. 2017).

Crossmodal Plasticity Occurred Across Multiple Layers of the Higher Order Sensory Cortices

Derived from the mean LFPs recorded simultaneously across the cortical thickness, the analysis of CSD sink amplitudes provided a measure of the current entering or leaving the neurons from the extracellular space through the cell membrane (Mitzdorf 1985; Einevoll et al. 2013). For each cortical region, averaged CSD waveforms were computed in the 2 groups (control vs. noise exposed) within each individual sink (i.e., supragranular, granular, infragranular-upper, and infragranular-lower layers) in response to the visual stimulus. Given the number of factors included in the present study, statistical analysis of the visual-evoked CSD sink amplitudes began with a 3-way repeated-measures ANOVA (group × cortical area × layer), which encompassed all of the data shown in Figure 4. As expected, this analysis yielded a significant interaction ($F[2.7,40.3] = 4.538$, $P < 0.01$). Due to the unique profile of each individual sink, subsequent statistical analyses were completed for each of the CSD sinks. Therefore, for each of the 4 panels in Figure 4 showing CSD sink amplitudes, a separate 2-way repeated-measures ANOVA (group × cortical area) was performed with Bonferroni post hoc tests (adjusted *P*-value = 0.013).

Overall, we observed an increased level of postsynaptic activity in response to visual stimulation within multiple cortical regions and their distinct layers 2 weeks after noise exposure; findings consistent with crossmodal plasticity following partial

hearing loss. Separate 2-way repeated-measures ANOVAs of the CSD sink amplitudes revealed a significant interaction of group by cortical area in both the granular layer ($F[2.1,31.1] = 5.58$, $P < 0.01$) as well as the infragranular-upper layer ($F[2.0,29.6] = 4.989$, $P < 0.05$). Although the supragranular and infragranular-lower layers did not show a significant interaction between main effects, all cortical layers showed a main effect of area (supragranular: $F[1.8,24.1] = 80.7$, $P < 0.001$; granular: $F[2.1,31.1] = 56.8$, $P < 0.001$; infragranular-upper: $F[2.0,29.6] = 55.2$, $P < 0.001$; infragranular-lower: $F[1.6,24.1] = 43.6$, $P < 0.001$). As expected, visual-evoked CSD sink amplitudes within the primary visual cortex (V1) were not affected by noise-induced hearing loss in any cortical layer ($P > 0.05$). Conversely, noise-induced hearing loss caused a significant increase in visual-evoked CSD sink amplitudes within the supragranular ($P < 0.013$), granular ($P < 0.01$), and infragranular-upper ($P < 0.01$) layers of the multisensory zone of V2L (V2L-Mz). Similarly, the neighboring region of the V2L-Az, which predominantly responded to auditory stimuli in control rats, showed a noise-induced increase in visual-evoked CSD sink amplitude within the granular ($P < 0.01$) and infragranular-upper ($P < 0.05$) layers. Taken together, these results reveal for the first time that hearing loss-induced crossmodal plasticity was not restricted to a single layer of the higher order sensory cortices.

Central Gain Enhancement was Layer-Specific and did not Extend Beyond the Auditory Cortex

Averaged CSD waveforms in response to auditory stimuli were also computed for the 2 groups within each of the 4 identified sinks (i.e., supragranular, granular, infragranular-upper, and infragranular-lower layers). Statistical analyses of the auditory-evoked CSD sink amplitudes began with a 3-way repeated-measures ANOVA, which revealed a significant interaction ($F[2.7,40.4] = 10.9$, $P < 0.001$) of group by cortical area by layer (Fig. 5). Thus, subsequent analyses were completed for each of the 4 individual CSD sinks, whereby a separate 2-way repeated-measures ANOVA (group × cortical area) was performed with Bonferroni post hoc tests (adjusted P-value = 0.013) for each of the 4 bar graphs presented in Fig. 5.

Auditory-evoked CSD sink amplitudes showed differential changes across the neighboring cortical regions following noise exposure, as evidenced by significant interactions of group by cortical area in both the granular layer ($F[2.0,30.0] = 12.04$, $P < 0.001$) and infragranular-upper layer ($F[1.9,28.9] = 11.7$, $P < 0.001$) (Fig. 5; 2-way repeated-measures ANOVAs). Furthermore, despite accounting for noise-induced hearing loss by adjusting the sound level of the auditory stimulus to be 40 dB above each rat's click threshold, the auditory-evoked CSD sink amplitudes were reduced across multiple layers in the audiovisual cortex of noise exposed rats. More specifically, within the multisensory zone of the V2L, noise exposure caused a significant decrease in the auditory-evoked CSD sink amplitude in the supragranular layer (control 0.56 mV/mm^2 vs. noise exposed 0.38 mV/mm^2, $P < 0.001$), granular layer (control 2.68 mV/mm^2 vs. noise exposed 1.11 mV/mm^2, $P < 0.001$), and infragranular-upper layer (control 2.23 mV/mm^2 vs. noise exposed 1.04 mV/mm^2, $P < 0.001$) (V2L-Mz; Fig. 5). Similarly, the auditory zone of the V2L showed a decrease in auditory-evoked CSD sink amplitude within the granular layer ($P = 0.034$) and infragranular-upper layer ($P < 0.01$) (V2L-Az; Fig. 5). A drastically different profile, however, emerged within the granular layer of the neighboring auditory cortex, AuD (control 4.69 mV/mm^2 vs. noise exposed 7.77 mV/mm^2, $P < 0.01$; Fig. 5). To summarize, unlike the observed reduction in the net positive current entering the neurons in the granular layer of the audiovisual cortex (V2L-Az), the CSD sink amplitude in AuD increased following noise exposure; findings consistent with central gain enhancement in this higher order auditory area.

Noise Exposure Caused a Differential Effect on AVREC Peak Amplitude in the Auditory, Visual and Audiovisual Cortices

As a complement to the comparisons performed on individual CSD sinks, AVREC waveforms were computed for each of the 4 cortical regions in response to the separately presented auditory and visual stimuli. These results were then compared between groups to provide an assessment of whether noise exposure changed the overall activation of postsynaptic currents in the different cortices (Fig. 6). An initial 3-way repeated-measures ANOVA revealed a significant interaction of group by cortical area by stimulus ($F[3,45] = 10.6$, $P < 0.001$) for the AVREC peak amplitude. Consequently, for each of the unimodal stimulus conditions (i.e., visual, Fig. 6A; auditory, Fig. 6B), a separate 2-way repeated measures ANOVA (group × cortical area) was performed with Bonferroni post hoc tests (adjusted P-value = 0.013).

Consistent with the associated CSD profiles, noise exposure caused differential changes in the AVREC peak amplitude in the visual (V1), auditory (AuD) and audiovisual cortices (V2L-Mz; V2L-Az), whereby the nature and extent of this plasticity depended on the stimulus modality presented (Fig. 6). For example, in response to visual stimulation (Fig. 6A), an increase in AVREC peak amplitude was observed within the multisensory zone of V2L (V2L-Mz, $P = 0.018$), the auditory zone of V2L (V2L-Az; $P < 0.01$) and the dorsal auditory cortex (AuD; $P < 0.01$). There was no significant 2-way interaction between the main effects of cortical area and group for visual-evoked AVREC peak amplitude ($F[1.8,27.2] = 3.35$, $P = 0.054$); however, there was a main effect of cortical area ($F[1.8,27.2] = 61.65$, $P < 0.001$). Thus, throughout the neighboring regions of the higher order sensory cortices, noise exposure induced crossmodal plasticity which was characterized by an increase in the overall activation of postsynaptic currents in response to visual stimuli (Fig. 6A).

The effect of noise-induced hearing loss on the auditory-evoked AVREC peak amplitude was also examined in the 4 cortical regions (Fig. 6B). Despite accounting for each rat's hearing sensitivity, a 2-way repeated measures ANOVA found a significant interaction of group by cortical area ($F[1.9,29.2] = 13.9$, $P < 0.001$) on the auditory-evoked AVREC peak amplitude. Furthermore, compared with the controls, post hoc testing revealed that the noise exposed rats had a significant decrease in AVREC peak amplitude in response to auditory stimulation within the audiovisual cortex (e.g., V2L-Mz $P < 0.001$; V2L-Az, $P < 0.013$). In stark contrast, the once-predominantly auditory region, AuD, showed a paradoxical increase (51 ± 17%) in its response to auditory stimulation following noise-induced hearing loss (AVREC peak amplitude: control 1.52 mV/mm^2 vs. noise exposed 2.21 mV/mm^2, $P = 0.014$; Fig. 6B); findings indicative of central gain enhancement. Collectively, these results further confirmed that noise-induced hearing loss caused the neighboring regions of the higher order sensory cortices to experience differential plasticity at the level of postsynaptic potentials.

Audiovisual Responsiveness was Preserved Despite the Coexistence of Central Gain Enhancement and Crossmodal Plasticity in Higher Order Sensory Cortices

In addition to the separately presented auditory and visual cues, we delivered these stimuli in combination to the noise exposed rats and age-matched controls in order to determine if

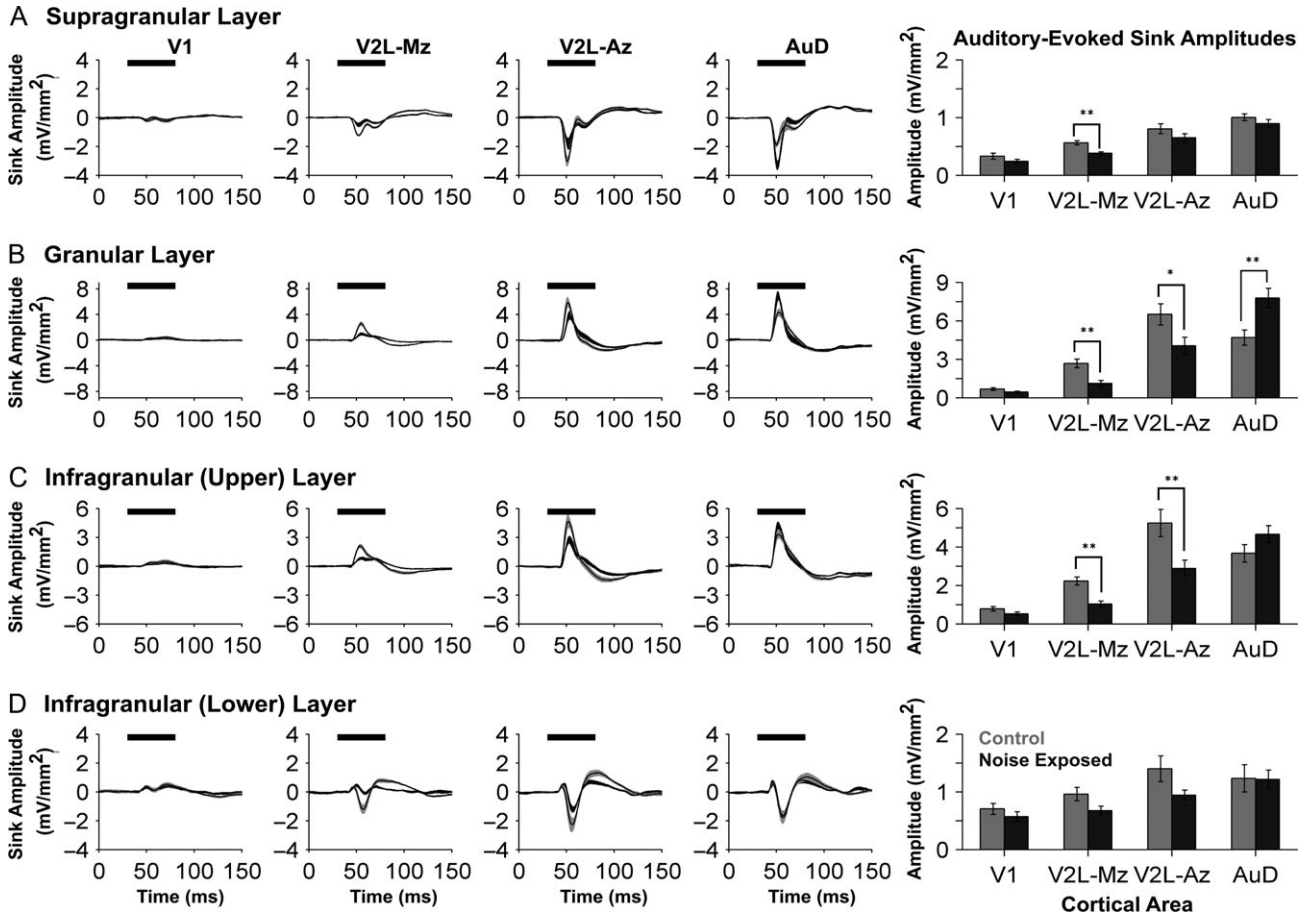

Figure 5. Noise-induced hearing loss caused region- and layer-specific plasticity in the auditory-evoked CSD profiles across auditory, visual and audiovisual cortices. Averaged CSD waveforms from supragranular (*A*), granular (*B*), infragranular-upper (*C*), and infragranular-lower (*D*) layers within all recording locations (i.e., V1, V2L-Mz, V2L-Az, and AuD; from left to right). The horizontal black bar denotes the presentation of the auditory stimulus, and the dark lines represent the group mean and shading represents the SEM for the noise exposed (dark grey; $n = 9$) and control (light grey; $n = 8$) groups. Consistent with Figure 4, the y-ordinate is specific to the waveform profile for each cortical layer. An analysis of auditory-evoked sink amplitudes (see bar graphs on the far right) shows a decrease in sink amplitude within V2L-Mz and V2L-Az, despite adjusting for individual rat differences in hearing sensitivity. Whereas both subregions of V2L demonstrated crossmodal plasticity (i.e., increased visual responsiveness and a commensurate decrease in auditory), their neighboring cortical region, AuD, showed a significant increase in auditory-evoked sink amplitude ($P < 0.01$), which was restricted to the granular layer. Values are mean ± SEM for the noise exposed ($n = 9$) and control ($n = 8$) groups. *$P < 0.05$; **$P < 0.013$.

audiovisual responsiveness was affected by adult-onset hearing loss. To that end, we used the granular sink and AVREC peak amplitudes to assess whether the actual responses to audiovisual stimuli deviated from the linear summation of the 2 unisensory responses. Based on this established approach (Laurienti et al. 2005; Lippert et al. 2013; Stein et al. 2009), we expected that the predominantly unisensory areas (V1 and AuD) in control rats would show a near-linear relationship between the actual (i.e., measured) response to the combined audiovisual stimuli and the predicted response (i.e., the sum of the separately presented auditory and visual stimuli). Furthermore, it was expected that the audiovisual regions of the lateral extrastriate visual cortex (V2L-Mz and V2L-Az) would instead show a sublinear relationship because the measured response to the combined audiovisual stimuli would be less than the summation of the 2 unisensory conditions; a finding which would be consistent with recordings in the multisensory cortices of various species (Meredith and Allman et al. 2012; Foxworthy et al. 2013).

Within the predominantly unisensory areas of control rats, AuD showed a near-linear interaction in which the measured response within the granular sink to the combined audiovisual stimuli was nearly equivalent to that of the predicted (summed) response (94.5 ± 2.9% of predicted), whereas V1 demonstrated a modest sublinear audiovisual interaction within the granular sink (85.8 ± 3.9% of predicted; Fig. 7A). As shown in Figure 7B, AVREC analyses revealed a similar trend within these 2 predominantly unisensory cortical regions, with the majority of the data from the control rats clustering along the line of unity (i.e., measured = predicted). Also consistent with our expectations for control rats, we observed that the multisensory zone of V2L (V2L-Mz) demonstrated the largest sublinear relationship, in which the measured response failed to approximate the predicted sum of the unisensory responses (granular sink: 78.6 ± 3.9% of predicted; AVREC peak amplitude: 75.1 ± 9.8% of predicted). Finally, the auditory zone of V2L (V2L-Az) of control rats showed a modest sublinear response (granular sink: 88.6 ± 3.7%; AVREC peak amplitude: 85.3 ± 2.7% of predicted).

Ultimately, to assess the effect of noise-induced hearing loss on audiovisual responsiveness, we compared whether the responses to audiovisual stimuli in the noise exposed rats deviated from the linear summation of the 2 unisensory responses to the same extent as was observed in the age-matched controls. Overall, a comparison of control versus noise exposed

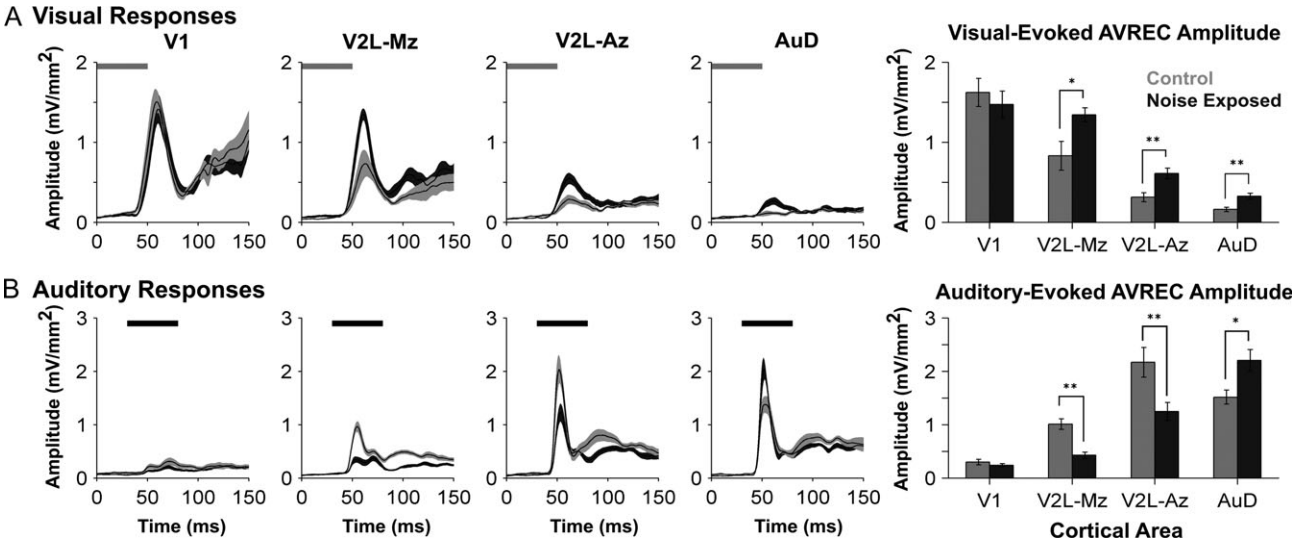

Figure 6. Neighboring cortical regions were differentially affected by noise-induced hearing loss as measured by the stimulus-evoked AVREC peak amplitudes. AVREC waveforms from V1, V2L-Mz, and V2L-Az, AuD (from left to right) in response to a visual (A) and auditory (B) stimulus. In response to visual stimulation (A), noise exposed rats (dark grey) showed increased AVREC peak amplitudes within subregions of the multisensory cortex (V2L-Mz and V2L-Az) as well as the neighboring dorsal auditory cortex (AuD). The horizontal grey and black bar denotes the presentation of the visual and auditory stimuli, respectively. In response to auditory stimulation (B), AVREC peak amplitudes were significantly reduced within the audiovisual cortex (V2L-Mz and V2L-Az) in noise exposed rats when compared with controls. Alternatively, noise exposed rats showed increased auditory-evoked activity within the dorsal auditory cortex (AuD). In the AVREC waveform plots, dark lines represent the group mean and shading represents the SEM for the noise exposed (dark grey; $n = 9$) and control (light grey; $n = 8$) groups. Values plotted in the bar graphs on the far right are mean ± SEM for the noise exposed ($n = 9$) and control ($n = 8$) groups. *$P < 0.05$; **$P < 0.013$.

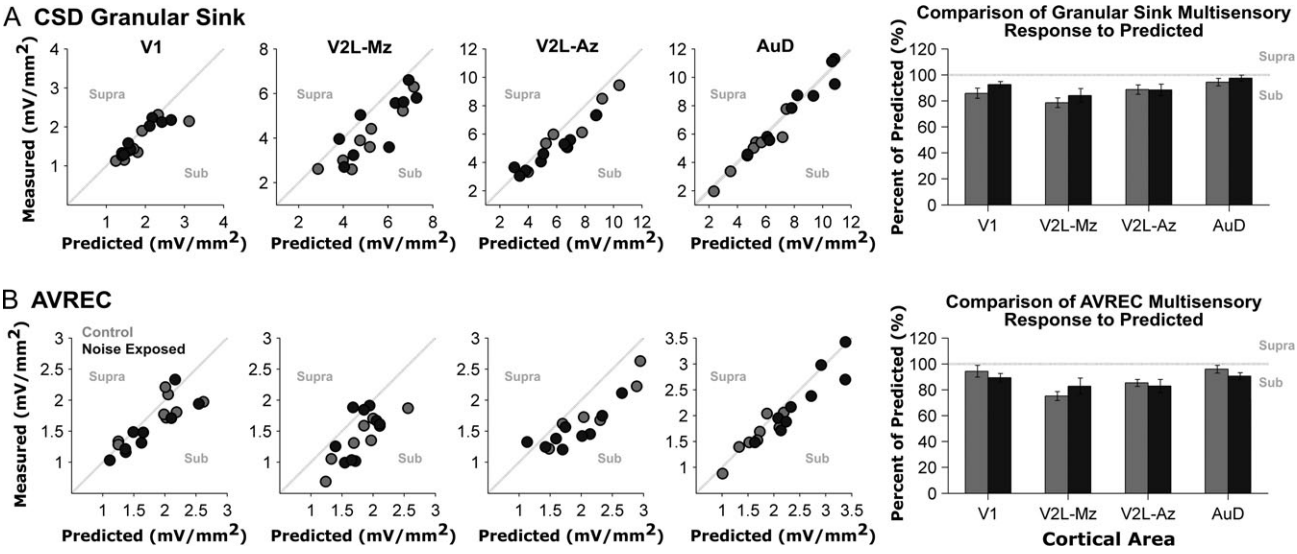

Figure 7. Audiovisual responsiveness was not affected by noise-induced hearing loss within the auditory, visual and audiovisual cortices. Quantification of audiovisual responsiveness was completed for each experiment by determining to what degree the measured audiovisual response deviated from the predicted (summed) response. For each recording location, the measured audiovisual granular sink amplitudes (A) and AVREC peak amplitudes (B) are plotted with respect to their predicted (summed) amplitude for control (grey dots, $n = 8$) and noise exposed rats (dark grey dots; $n = 9$). Responses within the primary visual (V1; far left) and dorsal auditory cortex (AuD; far right scatter plot) predominantly fall near the line of unity, as a result of the measured amplitude to the combined audiovisual stimuli being equivocal to the predicted sum of the separately presented auditory and visual stimuli. However, responses in the audiovisual cortex (V2L-Mz) were predominantly sublinear (i.e., below the line of unity), because the combined audiovisual response was smaller than the predicted sum. On each scatter plot, the words supra and sub describe the polarity of the response (i.e., responses that were greater- or lesser than the predicted sum were supra-additive or sub-additive, respectively). Overall, no significant differences were found between control and noise exposed groups for the granular sink or AVREC peak amplitudes across all recording locations.

rats showed no significant difference between groups for the granular sink or AVREC peak amplitude for all cortical areas ($P > 0.05$). Furthermore, there was no significant interaction between the main effects of cortical area and group for both the granular sink ($F[3,45] = 0.341$, $P = 0.80$) and AVREC peak amplitude ($F[3,45] = 0.916$, $P = 0.44$). There was, however, a main effect of cortical area for both the granular sink ($F[3,45] = 5.074$, $P < 0.01$) and AVREC peak amplitude ($F[3,45] = 4.391$, $P < 0.01$); findings which (not surprisingly) indicated that the cortical areas did indeed show a differential response to audiovisual

stimuli. Collectively, these results revealed that noise-induced hearing loss did not disrupt audiovisual responsiveness despite the coexistence of central gain enhancement and crossmodal plasticity in the higher order sensory cortices.

Discussion

In the present study, we conducted the first investigation of altered laminar processing in the auditory, visual and audiovisual cortices following adult-onset hearing loss. More specifically, we compared the auditory and visually evoked postsynaptic activity in noise exposed rats versus age-matched controls to assess the cortical region- and layer-specificity of central gain enhancement and crossmodal plasticity; 2 phenomena that were known to occur following hearing impairment, but had never been studied concurrently. LFP recordings and the subsequent CSD analyses revealed that central gain enhancement was restricted to the granular layer of the once-predominantly auditory area, AuD, whereas crossmodal plasticity—characterized by an increase in visual responsiveness—was evident across multiple layers of the audiovisual cortex (V2L) and extended into AuD. Surprisingly, despite these neighboring cortical regions showing differing degrees of central gain enhancement and crossmodal plasticity, noise-induced hearing loss did not disrupt their overall responsiveness to combined audiovisual stimuli. Taken together, our results have shown for the first time that the plasticity induced by partial hearing loss manifests differentially across the layers of neighboring regions of the higher order sensory cortices.

Cortical Region- and Layer-Specific Plasticity following Partial Hearing Loss

Noise-induced hearing loss resulted in both region- and layer-specific plasticity in the auditory (AuD) and audiovisual cortices (V2L-Mz and V2L-Az). As predicted, central gain enhancement occurred in the higher order auditory area, AuD, characterized by an increase in synaptic input as measured by the AVREC peak amplitude (Fig. 6). This heightened auditory-evoked activity in the AuD was consistent with the increase in evoked potentials observed previously in the core auditory cortex following loud noise exposure in rats (Popelar et al. 1995, 2008). Interestingly, central gain enhancement was not present across all layers of the AuD, as only the granular layer showed a significant increase in CSD sink amplitude (Fig. 5B). Unexpectedly, there was no evidence of a noise-induced increase in auditory activation within the subregions of the audiovisual cortex (V2L-Mz and V2L-Az). In fact, across these cortical layers, partial hearing loss caused a significant decrease in auditory-evoked CSD sink amplitudes (Fig. 5). The restricted emergence of central gain enhancement in only the higher order auditory cortex was surprising given that the audiovisual cortex in rodents (and other species) is known to receive extensive inputs from the auditory cortex (Budinger et al. 2000, 2006; Budinger and Scheich 2009; Laramée et al. 2011). Based on this areal convergence, we had predicted that the hyperexcitability observed in the auditory cortex would be relayed to the directly connected audiovisual areas; however, this was not the case. Thus, our results provide the first direct evidence that deprivation-induced central gain enhancement does not extend into the audiovisual cortex following partial hearing loss in adulthood.

Although the neighboring regions of the auditory and audiovisual cortices experienced differential changes in their auditory responsiveness postnoise exposure (i.e., increased in AuD vs. decreased in V2L), both cortical areas experienced crossmodal plasticity, whereby the overall strength of the postsynaptic currents (AVREC) increased in response to visual stimulation (Fig. 6). Based on these LFP-derived results, it is reasonable to expect that this amplified visual input to V2L and AuD would facilitate an increase in neuronal spiking responses following partial hearing loss. Indeed, in our previous mapping study, we reported that an increased proportion of neurons in the AuD and V2L of noise exposed rats showed spiking responses to visual stimulation compared with age-matched controls (Schormans and Typlt et al. 2017).

We are unaware of any human studies that have investigated the coexistence of central gain enhancement and crossmodal plasticity; however, there have been recent reports of altered auditory and visual processing in hearing-impaired adults. For example, using functional magnetic resonance imaging (fMRI), Puschmann and Thiel (2017) found that the severity of hearing loss in adults was associated with an increase in the functional connectivity between the auditory cortex and the motion-sensitive visual area MT during audiovisual processing. Furthermore, in a series of studies using passively elicited EEG responses and current source localization procedures, Campbell and Sharma found that the temporal cortex of adults with mild-moderate hearing loss showed a reduced activation to speech sounds (2013) and an increased activation to visual stimuli (2014). Moreover, because this passive listening caused an increased activation of frontal cortical regions in these hearing-impaired adults, it was suggested that, in addition to crossmodal plasticity, a re-allocation of cortical resources had occurred such that frontal areas were now tasked with supporting nonattentive auditory processing (Campbell and Sharma 2013). Ultimately, future studies will be needed to determine the long-term, functional consequences that follow the initial period of sensory reorganization observed in the present study. In addition to the suggestion to use longitudinal studies to track the progression of hearing loss-induced changes in audiovisual processing (Musacchia et al. 2009; Campbell and Sharma 2014), it will also be important to determine how the severity of hearing loss impacts the emergence and persistence of central gain enhancement and crossmodal plasticity in hearing-impaired adults.

Putative Mechanisms of Central Gain Enhancement and Crossmodal Plasticity

At present, the structural and/or physiological changes contributing to central gain enhancement and crossmodal plasticity have not been fully elucidated. Because we have shown that these phenomena can coexist following partial hearing loss, it is worth considering whether they share putative mechanisms. It has been proposed that central gain enhancement (Auerbach et al. 2014) and crossmodal plasticity (Nys et al. 2015) may arise from a loss of intracortical inhibition, which is perhaps not surprising given that noise exposure is known to alter the balance of excitation and inhibition in cortical circuits (Yang et al. 2011). In addition, it has long been suggested that an unmasking of inputs could lead to cortical crossmodal plasticity following sensory deprivation (Rauschecker 1995), and it was recently proposed that central gain enhancement might represent an emergent property of altered network activity due to unmasked synaptic connections (Auerbach et al. 2014). Indeed, the upscaling of excitatory synapses via homeostatic plasticity mechanisms could increase the strength of previously subthreshold inputs following sensory deprivation (Lee 2012; Lee and Whitt 2015). That said, because the majority of studies investigating homeostatic mechanisms associated with crossmodal plasticity have used models of complete sensory loss (for review, see Whitt et al. 2014), future studies are

needed to determine whether partial hearing loss is sufficient to cause crossmodal plasticity (and/or central gain enhancement) via synaptic scaling.

It is important to note that the mechanisms underlying central gain enhancement and crossmodal plasticity need not be constrained to intrinsic changes in the cortex. For example, cortical crossmodal plasticity could manifest from altered multisensory processing in subcortical areas that becomes effectively relayed to the impaired cortex (Allman et al. 2009; Laramée et al. 2011; Mezzera and López-Bendito 2015). Interestingly, we observed that the changes induced by partial hearing loss were not restricted to processing within the supragranular/infragranular layers, as the granular CSD sink amplitudes were also greatly affected (Fig. 5B). More specifically, within the audiovisual cortex (V2L-Mz and V2L-Az), there was an increased response to visual stimulation, coupled with reduced input during auditory stimulation (Fig. 4B). At the same time, increased auditory activation was restricted to the granular layer; indicative of central gain enhancement within the neighboring auditory area, AuD (Fig. 5B). Taken together, these results identify the potential contribution of thalamocortical projections to both central gain enhancement and cortical crossmodal plasticity following a modest hearing loss. Ultimately, because a previous study found that exposure to complete deafness for 6–8 days potentiated thalamocortical synapses in the primary visual cortex but not in the primary auditory cortex of mice (Petrus et al. 2014), future studies are warranted to explore the contribution of thalamocortical plasticity following partial hearing loss.

Audiovisual Processing and Partial Hearing Loss

In addition to revealing that noise-induced central gain enhancement and crossmodal plasticity were not mutually exclusive phenomena, we also investigated whether partial hearing loss affected the responsiveness of the higher order sensory cortices to combined audiovisual stimulation. Of the neighboring cortical regions in control rats, the multisensory zone of the V2L (V2L-Mz) showed the largest degree of audiovisual processing as assessed by an established metric of additivity (see Methods; Laurienti et al. 2005; Lippert et al. 2013; Stein et al. 2009). As expected in control rats, we observed that the responsiveness of the V2L-Mz to the combined audiovisual stimulation failed to match the sum of the separately presented auditory and visual stimuli (i.e., there was a sublinear relationship; Fig. 7). At the same time, the AuD of control rats showed a near-linear relationship; findings which indicated that visual stimulation had a limited effect on auditory processing in this predominantly auditory area prior to hearing loss. Surprisingly, despite partial hearing loss causing both central gain enhancement and crossmodal plasticity, the relationships between the actual (measured) versus predicted (summed) responses were preserved in the neighboring regions of their higher order sensory cortices, such that the noise exposed rats showed the same degree of audiovisual additivity as the age-matched controls (Fig. 7). At this time, it is unclear how this preservation of audiovisual responsiveness in the presence of layer-specific central gain enhancement and crossmodal plasticity, ultimately impacts audiovisual perception.

To date, only a few studies in humans have investigated how partial hearing loss affects audiovisual processing and multisensory integration, and the results suggest potential disparity between the subjects' behavioral performance versus the associated cortical activity. For example, during tasks requiring participant perceptual reporting, audiovisual integration of speech stimuli was similar between older adults with mild-moderate hearing impairment compared with normal-hearing listeners of the same age (Tye-Murray et al. 2007) or younger (Başkent and Bazo 2011). In contrast, compared with age-matched controls, older adults with hearing loss showed degraded audiovisual integration as assessed with cortical evoked potentials elicited by watching and listening to speech stimuli (Musacchia et al. 2009).

Given that it is possible to train laboratory animals, including rodents, to perform complex audiovisual tasks (Sakata et al. 2004; Hirokawa et al. 2008; Gleiss and Kayser 2012; Raposo et al. 2012; Siemann et al. 2015; Schormans and Scott et al. 2017), we suggest that coupling electrophysiological recordings with behavioral studies could help to elucidate the effect of adult-onset hearing loss on audiovisual processing and perception. Using such models, it would be possible to determine the degree to which the adult brain is capable of compensating for hearing impairment, and by extension, the severity of hearing loss that ultimately results in a failure to accurately integrate audiovisual stimuli. Guided by the results of the present study, our future work will seek to uncover the perceptual implications of the complex assortment of the hearing loss-induced intramodal and crossmodal changes that occur across the layers of the higher order sensory cortices.

Funding

Natural Sciences and Engineering Research Council of Canada (NSERC Discovery Grant 435819-2013 RGPIN to B.L.A.) and the Canadian Institutes of Health Research (CIHR 137098 to B.L.A.).

Notes

We would like to acknowledge Daniel Stolzberg (University of Western Ontario) for his assistance with current-source density analysis. *Conflict of Interest: None declared*.

References

Agrawal Y, Platz EA, Niparko JK. 2008. Prevalence of hearing loss and differences by demographic characteristics among us adults: Data from the national health and nutrition examination survey, 1999–2004. Arch Intern Med. 168: 1522–1530.

Allman BL, Bittencourt-Navarrete RE, Keniston LP, Medina AE, Wang MY, Meredith MA. 2008. Do cross-modal projections always result in multisensory integration? Cereb Cortex. 18: 2066–2076.

Allman BL, Keniston LP, Meredith MA. 2009. Adult deafness induces somatosensory conversion of ferret auditory cortex. Proc Natl Acad Sci. 106:5925–5930.

Allman BL, Meredith MA. 2007. Multisensory processing in "unimodal" neurons: cross-modal subthreshold auditory effects in cat extrastriate visual cortex. J Neurophysiol. 98: 545–549.

Auer ET, Bernstein LE, Sungkarat W, Singh M. 2007. Vibrotactile activation of the auditory cortices in deaf versus hearing adults. NeuroReport. 18:645–648.

Auerbach BD, Rodrigues PV, Salvi RJ. 2014. Central gain control in tinnitus and hyperacusis. Front Neurol. 5:206.

Barth DS, Goldberg N, Brett B, Di S. 1995. The spatiotemporal organization of auditory, visual, and auditory-visual evoked potentials in rat cortex. Brain Res. 678:177–190.

Başkent D, Bazo D. 2011. Audiovisual asynchrony detection and speech intelligibility in noise with moderate to severe sensorineural hearing impairment. Ear Hear. 32:582–592.

Budinger E, Heil P, Hess A, Scheich H. 2006. Multisensory processing via early cortical stages: connections of the primary auditory cortical field with other sensory systems. Neuroscience. 143:1065–1083.

Budinger E, Heil P, Scheich H. 2000. Functional organization of auditory cortex in the Mongolian gerbil (Meriones unguiculatus). III. Anatomical subdivisions and corticocortical connections. Eur J Neurosci. 12:2425–2451.

Budinger E, Scheich H. 2009. Anatomical connections suitable for the direct processing of neuronal information of different modalities via the rodent primary auditory cortex. Hear Res. 258:16–27.

Campbell J, Sharma A. 2013. Compensatory changes in cortical resource allocation in adults with hearing loss. Front Syst Neurosci. 7:71.

Campbell J, Sharma A. 2014. Cross-modal re-organization in adults with early stage hearing loss. PLoS One. 9(2):e90594.

Doucet ME, Bergeron F, Lassonde M, Ferron P, Lepore F. 2006. Cross-modal reorganization and speech perception in cochlear implant users. Brain. 129:3376–3383.

Einevoll GT, Kayser C, Logothetis NK, Panzeri S. 2013. Modelling and analysis of local field potentials for studying the function of cortical circuits. Nat Rev Neurosci. 14:770–785.

Engineer ND, Riley JR, Seale JD, Vrana WA, Shetake JA, Sudanagunta SP, Borland MS, Kilgard MP. 2011. Reversing pathological neural activity using targeted plasticity. Nature. 470:101.

Finney EM, Clementz BA, Hickok G, Dobkins KR. 2003. Visual stimuli activate auditory cortex in deaf subjects: evidence from MEG. NeuroReport. 14:1425–1427.

Finney EM, Fine I, Dobkins KR. 2001. Visual stimuli activate auditory cortex in the deaf. Nat Neurosci. 4:1171–1173.

Foxworthy WA, Allman BL, Keniston LP, Meredith MA. 2013. Multisensory and unisensory neurons in ferret parietal cortex exhibit distinct functional properties. Eur J Neurosci. 37:910–923.

Freeman B, Singer W. 1983. Direct and indirect visual inputs to superficial layers of cat superior colliculus: a current source-density analysis of electrically evoked potentials. J Neurophysiol. 49:1075–1091.

Givre SJ, Schroeder CE, Arezzo JC. 1994. Contribution of extrastriate area V4 to the surface-recorded flash VEP in the awake macaque. Vision Res. 34:415–428.

Gleiss S, Kayser C. 2012. Audio-visual detection benefits in the rat. PLoS One. 7:e45677.

Happel MFK, Jeschke M, Ohl FW. 2010. Spectral integration in primary auditory cortex attributable to temporally precise convergence of thalamocortical and intracortical input. J Neurosci. 30:11114–11127.

Hirokawa J, Bosch M, Sakata S, Sakurai Y, Yamamori T. 2008. Functional role of the secondary visual cortex in multisensory facilitation in rats. Neuroscience. 153:1402–1417.

Hunt DL, Yamoah EN, Krubitzer L. 2006. Multisensory plasticity in congenitally deaf mice: How are cortical areas functionally specified? Neuroscience. 139:1507–1524.

Komiya H, Eggermont JJ. 2000. Spontaneous firing activity of cortical neurons in adult cats with reorganized tonotopic map following pure-tone trauma. Acta Otolaryngol (Stockh.). 120:750–756.

Kral A, Eggermont JJ. 2007. What's to lose and what's to learn: development under auditory deprivation, cochlear implants and limits of cortical plasticity. Brain Res Rev. 56:259–269.

Kral A, Schröder J-H, Klinke R, Engel AK. 2003. Absence of cross-modal reorganization in the primary auditory cortex of congenitally deaf cats. Exp Brain Res. 153:605–613.

Kujawa SG, Liberman MC. 2009. Adding insult to injury: cochlear nerve degeneration after "temporary" noise-induced hearing loss. J Neurosci. 29:14077–14085.

Laramée ME, Kurotani T, Rockland KS, Bronchti G, Boire D. 2011. Indirect pathway between the primary auditory and visual cortices through layer V pyramidal neurons in V2L in mouse and the effects of bilateral enucleation. Eur J Neurosci. 34:65–78.

Laurienti PJ, Perrault TJ, Stanford TR, Wallace MT, Stein BE. 2005. On the use of superadditivity as a metric for characterizing multisensory integration in functional neuroimaging studies. Exp Brain Res. 166:289–297.

Lee H-K. 2012. Ca-permeable AMPA receptors in homeostatic synaptic plasticity. Front Mol Neurosci. 5:17.

Lee H-K, Whitt JL. 2015. Cross-modal synaptic plasticity in adult primary sensory cortices. Curr Opin Neurobiol. 35:119–126.

Lin HW, Furman AC, Kujawa SG, Liberman MC. 2011. Primary neural degeneration in the guinea pig cochlea after reversible noise-induced threshold shift. J Assoc Res Otolaryngol. 12:605–616.

Lippert MT, Takagaki K, Kayser C, Ohl FW. 2013. Asymmetric multisensory interactions of visual and somatosensory responses in a region of the rat parietal cortex. PLoS One. 8: e63631.

Lomber SG, Meredith MA, Kral A. 2010. Cross-modal plasticity in specific auditory cortices underlies visual compensations in the deaf. Nat Neurosci. 13:1421–1427.

Meredith MA, Allman BL, Keniston LP, Clemo HR. 2012. Are bimodal neurons the same throughout the brain? In: Murray MM, Wallace MT, editors. The neural bases of multisensory processes. Boca Raton, FL: CRC Press. p. 51–64.

Meredith MA, Allman BL. 2009. Subthreshold multisensory processing in cat auditory cortex. NeuroReport. 20:126–131.

Meredith MA, Allman BL. 2015. Single-unit analysis of somatosensory processing in the core auditory cortex of hearing ferrets. Eur J Neurosci. 41:686–698.

Meredith MA, Keniston LP, Allman BL. 2012. Multisensory dysfunction accompanies crossmodal plasticity following adult hearing impairment. Neuroscience. 214:136–148.

Meredith MA, Kryklywy J, McMillan AJ, Malhotra S, Lum-Tai R, Lomber SG. 2011. Crossmodal reorganization in the early deaf switches sensory, but not behavioral roles of auditory cortex. Proc Natl Acad Sci. 108:8856–8861.

Meredith MA, Lomber SG. 2011. Somatosensory and visual crossmodal plasticity in the anterior auditory field of early-deaf cats. Hear Res. 280:38–47.

Mezzera C, López-Bendito G. 2016. Cross-modal plasticity in sensory deprived animal models: from the thalamocortical development point of view. J Chem Neuroanat. 17:32–40.

Mitzdorf U. 1985. Current source-density method and application in cat cerebral cortex: investigation of evoked potentials and EEG phenomena. Physiol Rev. 65:37–100.

Mitzdorf U, Singer W. 1977. Laminar segregation of afferents to lateral geniculate nucleus of the cat: an analysis of current source density. J Neurophysiol. 40:1227–1244.

Mitzdorf U, Singer W. 1980. Monocular activation of visual cortex in normal and monocularly deprived cats: an analysis of evoked potentials. J Physiol. 304:203–220.

Musacchia G, Arum L, Nicol T, Garstecki D, Kraus N. 2009. Audiovisual deficits in older adults with hearing loss: biological evidence. Ear Hear. 30:505–514.

Nicholson C, Freeman JA. 1975. Theory of current source-density analysis and determination of conductivity tensor for anuran cerebellum. J Neurophysiol. 38:356–368.

Nys J, Smolders K, Laramée M-E, Hofman I, Hu T-T, Arckens L. 2015. Regional specificity of GABAergic regulation of cross-modal plasticity in mouse visual cortex after unilateral enucleation. J Neurosci. 35:11174–11189.

Paxinos G, Watson C. 2007. The rat brain in stereotaxic coordinates. Burlington, MA: Elsevier Inc.

Petrus E, Isaiah A, Jones AP, Li D, Wang H, Lee H-K, Kanold PO. 2014. Crossmodal induction of thalamocortical potentiation leads to enhanced information processing in the auditory cortex. Neuron. 81:664–673.

Popelar J, Grecova J, Rybalko N, Syka J. 2008. Comparison of noise-induced changes of auditory brainstem and middle latency response amplitudes in rats. Hear Res. 245:82–91.

Popelar J, Hartmann R, Syka J, Klinke R. 1995. Middle latency responses to acoustical and electrical stimulation of the cochlea in cats. Hear Res. 92:63–77.

Popelar J, Syka J, Berndt H. 1987. Effect of noise on auditory evoked responses in awake guina pigs. Hear Res. 26:239–247.

Popescu MV, Polley DB. 2010. Monaural deprivation disrupts development of binaural selectivity in auditory midbrain and cortex. Neuron. 65:718–731.

Raposo D, Sheppard JP, Schrater PR, Churchland AK. 2012. Multisensory decision-making in rats and humans. J Neurosci. 32:3726–3735.

Rauschecker JP. 1995. Compensatory plasticity and sensory substitution in the cerebral cortex. Trends Neurosci. 18:36–43.

Sakata S, Yamamori T, Sakurai Y. 2004. Behavioral studies of auditory-visual spatial recognition and integration in rats. Exp Brain Res. 159:409–417.

Salvi RJ, Saunders SS, Gratton MA, Arehole S, Powers N. 1990. Enhanced evoked response amplitudes in the inferior colliculus of the chinchilla following acoustic trauma. Hear Res. 50:245–257.

Salvi RJ, Wang J, Ding D. 2000. Auditory plasticity and hyperactivity following cochlear damage. Hear Res. 147:261–274.

Schormans AL, Scott KE, Vo AMQ, Tyker A, Typlt M, Stolzberg D, Allman BL. 2017. Audiovisual temporal processing and synchrony perception in the rat. Front Behav Neurosci. 10:246.

Schormans AL, Typlt M, Allman BL. 2017. Crossmodal plasticity in auditory, visual and multisensory cortical areas following noise-induced hearing loss in adulthood. Hear Res. 343: 92–107.

Schroeder CE, Javitt DC, Steinschneider M, Mehta AD, Givre SJ Jr, Vaughan HG, Arezzo JC. 1997. N-methyl-d-aspartate enhancement of phasic responses in primate neocortex. Exp Brain Res. 114:271–278.

Schroeder CE, Lindsley RW, Specht C, Marcovici A, Smiley JF, Javitt DC. 2001. Somatosensory input to auditory association cortex in the macaque monkey. J Neurophysiol. 85:1322–1327.

Schroeder CE, Mehta AD, Givre SJ. 1998. A spatiotemporal profile of visual system activation revealed by current source density analysis in the awake macaque. Cereb Cortex. 8: 575–592.

Siemann JK, Muller CL, Bamberger G, Allison JD, Veenstra-VanderWeele J, Wallace MT. 2015. A novel behavioral paradigm to assess multisensory processing in mice. Front Behav Neurosci. 8:456.

Stein BE, Stanford TR, Ramachandran R, Perrault TJ, Rowland BA. 2009. Challenges in quantifying multisensory integration: alternative criteria, models, and inverse effectiveness. Exp Brain Res. 198:113.

Stolzberg D, Chrostowski M, Salvi RJ, Allman BL. 2012. Intracortical circuits amplify sound-evoked activity in primary auditory cortex following systemic injection of salicylate in the rat. J Neurophysiol. 108:200–214.

Szymanski FD, Garcia-Lazaro JA, Schnupp JWH. 2009. Current source density profiles of stimulus-specific adaptation in rat auditory cortex. J Neurophysiol. 102:1483–1490.

Tye-Murray N, Sommers M, Spehar B. 2007. Audiovisual integration and lipreading of older adults with normal and impaired hearing. Ear Hear. 28:656–668.

Vachon P, Voss P, Lassonde M, Leroux J-M, Mensour B, Beaudoin G, Bourgouin P, Lepore F. 2013. Reorganization of the auditory, visual and multimodal areas in early deaf individuals. Neuroscience. 245:50–60.

Wallace MT, Ramachandran R, Stein BE. 2004. A revised view of sensory cortical parcellation. Proc Natl Acad Sci U S A. 101: 2167–2172.

Whitt JL, Petrus E, Lee H-K. 2014. Experience-dependent homeostatic synaptic plasticity in neocortex. Neuropharmacology. 78:45–54.

Xu J, Sun X, Zhou X, Zhang J, Yu L. 2014. The cortical distribution of multisensory neurons was modulated by multisensory experience. Neuroscience. 272:1–9.

Yang S, Weiner BD, Zhang LS, Cho S-J, Bao S. 2011. Homeostatic plasticity drives tinnitus perception in an animal model. Proc Natl Acad Sci. 108:14974–14979.